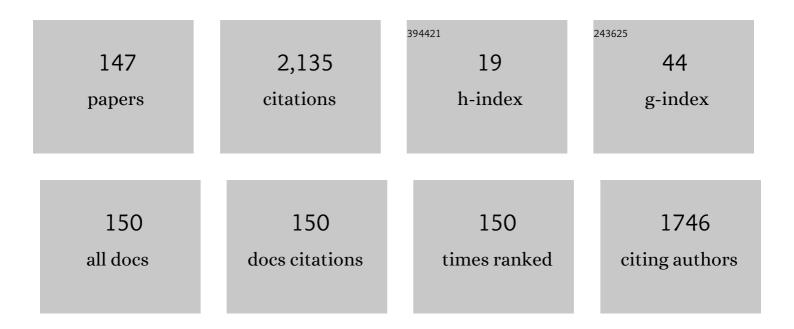
## Akinobu Yamaguchi

List of Publications by Year in descending order

Source: https://exaly.com/author-pdf/3196397/publications.pdf Version: 2024-02-01



#	Article	IF	CITATIONS
1	Observation of frequency dependent resonances in magnetic vortex core gyration using time-resolved magneto-optical Kerr microscope with pulsed semiconductor laser illumination. Japanese Journal of Applied Physics, 2022, 61, 018001.	1.5	1
2	Physically unclonable functions taggant for universal steganographic prints. Scientific Reports, 2022, 12, 985.	3.3	8
3	<i>In situ</i> fluorescence yield soft X-ray absorption spectroscopy of electrochemical nickel deposition processes with and without ethylene glycol. RSC Advances, 2022, 12, 10425-10430.	3.6	1
4	Physical stability of stealth nanobeacon using surface-enhanced Raman scattering for anti-counterfeiting and monitoring medication adherence: Deposition on various coating tablets. International Journal of Pharmaceutics, 2022, 624, 121980.	5.2	6
5	Highly stable and reproducible Au nanorod arrays for near-infrared optofluidic SERS sensor. Materials Letters, 2021, 286, 129106.	2.6	9
6	Non-Destructive Imaging on Synthesised Nanoparticles. Materials, 2021, 14, 613.	2.9	6
7	Direct observation of a magnetic domain change in Ni wire and film on a LiNbO3 substrate using X-ray magnetic circular dichroic photoemission electron microscopy. Japanese Journal of Applied Physics, 2021, 60, SBBC01.	1.5	2
8	Anisotropic pyrochemical dry etching of fluorinated ethylene propylene induced by pre-irradiation with synchrotron radiation. AIP Advances, 2021, 11, .	1.3	2
9	X-ray Photoemission Spectroscopy Study of Uniaxial Magnetic Anisotropy Induced in a Ni Layer Deposited on a LiNbO3 Substrate. Nanomaterials, 2021, 11, 1024.	4.1	1
10	Investigating R&D Committee on Magnetic Sensors for High-Performance and Systemization. IEEJ Transactions on Fundamentals and Materials, 2021, 141, 443-445.	0.2	0
11	Design and Fabrication of PTFE Substrate Integrated Waveguide Coupler by SR Direct Etching. IEICE Transactions on Electronics, 2021, E104.C, 446-454.	0.6	2
12	Enhancement of spin–orbit torques by change in uniaxial in-plane magnetic anisotropy of Py/Pt bilayers on single crystal 128° Y-Cut LiNbO3 substrate. Applied Physics Letters, 2021, 119, 152407.	3.3	0
13	Study on Fabrication of X-ray Collimators by X-ray Lithography Using Synchrotron Radiation. Journal of Photopolymer Science and Technology = [Fotoporima Konwakai Shi], 2021, 34, 213-218.	0.3	2
14	Liquid Mixing Evaluated Using Entropy in a Lab-on-a-disc Platform. Sensors and Materials, 2021, 33, 4371.	0.5	3
15	Fabrication of Ni–W Microgears Using LIGA Process. Sensors and Materials, 2021, 33, 4455.	0.5	4
16	A lab in a bento box: an autonomous centrifugal microfluidic system for an enzyme-linked immunosorbent assay. Analytical Methods, 2020, 12, 4858-4866.	2.7	7
17	X-ray absorption and photoemission spectroscopy of bulk insulating materials using graphene. Journal of Applied Physics, 2020, 128, .	2.5	4
18	Gold Nanoparticles Enhance EGFR Inhibition and Irradiation Effects in Head and Neck Squamous Carcinoma Cells. BioMed Research International, 2020, 2020, 1-10.	1.9	11

Акілови Үамадисні

#	Article	IF	CITATIONS
19	On chip synthesis of Au nanoparticles by microwave heating. Electronics and Communications in Japan, 2020, 103, 49-55.	0.5	2
20	Dependence of Gilbert damping constant on microstructure in nanocrystalline YIG coatings prepared by co-precipitation and spin-coating on a Si substrate. Journal of Magnetism and Magnetic Materials, 2020, 513, 167253.	2.3	19
21	Design of Microwave Applicator with Plural Microchannels Using Post-Wall Waveguide. , 2020, , .		ο
22	Application of microprobe soft X-ray fluorescence and absorption spectroscopic analyses to characterize the buried multi-layered micro-structure. Japanese Journal of Applied Physics, 2020, 59, 060902.	1.5	5
23	Solid/liquid-interface-dependent synthesis and immobilization of copper-based particles nucleated by X-ray-radiolysis-induced photochemical reaction. Journal of Synchrotron Radiation, 2020, 27, 1008-1014.	2.4	6
24	Study on relatively large response of rectifying voltage in Ni wires fabricated on a LiNbO <sub>3</sub> substrate. Japanese Journal of Applied Physics, 2020, 59, 083001.	1.5	0
25	Visualization of elemental distributions and local analysis of element-specific chemical states of an Arachnoidiscus sp. frustule using soft X-ray spectromicroscopy. PLoS ONE, 2020, 15, e0243874.	2.5	3
26	On Chip Synthesis of Au Nanoparticles by Microwave Heating. IEEJ Transactions on Electronics, Information and Systems, 2020, 140, 471-475.	0.2	0
27	Mixing of Different Density Liquids by Euler-force on Lab-on-a-disc. IEEJ Transactions on Electronics, Information and Systems, 2020, 140, 465-470.	0.2	0
28	Molecular Structure Evaluation of Bulk Polytetrafluoroethylene Modified by X-ray Irradiation. Journal of Photopolymer Science and Technology = [Fotoporima Konwakai Shi], 2020, 33, 295-299.	0.3	2
29	X-ray radiolysis-based three dimensional additive manufacturing process. , 2019, , .		0
30	Deep X-ray lithography system with a uniform and high-accuracy fabrication area established in beamline BL11 at NewSUBARU. Journal of Synchrotron Radiation, 2019, 26, 528-534.	2.4	11
31	Study on three dimensional additive manufacturing process using X-ray radiolysis. , 2019, , .		0
32	Deposition of Polytetrafluoroethylene Film Assisted by Synchrotron Radiation Irradiation. Journal of Photopolymer Science and Technology = [Fotoporima Konwakai Shi], 2019, 32, 249-252.	0.3	3
33	Present status of photoemission electron microscope newly installed in SPring-8 for time-resolved nanospectroscopy. Japanese Journal of Applied Physics, 2019, 58, 118001.	1.5	7
34	Anisotropic Pyrochemical Etching of PTFE by Synchrotron Radiation. , 2019, , .		0
35	The Study on Magnetization Reversal of Stripe-Domain Structure in Ni Wires Fabricated on a LiNbO3 Substrate. IEEE Transactions on Magnetics, 2019, 55, 1-4.	2.1	1
36	Quasi-free-standing monolayer hexagonal boron nitride on Ni. Materials Research Express, 2019, 6, 016304.	1.6	1

#	Article	IF	CITATIONS
37	Aggregation and dispersion of Au-nanoparticle-decorated polystyrene beads with SERS-activity using AC electric field and Brownian movement. Applied Surface Science, 2019, 465, 405-412.	6.1	9
38	Controllability of cupric particle synthesis by linear alcohol chain number as additive and pH control in cupric acetate solution using X-ray radiolysis. Journal of Synchrotron Radiation, 2019, 26, 1986-1995.	2.4	8
39	Magnetic Scattering in Ni Wires Fabricated on Ferroelectric LiNbO3 Substrate for Magnetic Sensor Application. Sensors and Materials, 2019, 31, 3007.	0.5	4
40	X-ray Radiolysis-based Three Dimensional Additive Manufacturing Process. Transactions of the Japan Institute of Electronics Packaging, 2019, 12, E19-003-1-E19-003-7.	0.4	3
41	Modification of the Transmittance of Bulk Polytetrafluoroethylene via Synchrotron Radiation Irradiation. Journal of Photopolymer Science and Technology = [Fotoporima Konwakai Shi], 2019, 32, 253-256.	0.3	4
42	Ferromagnetic resonance of Ni wires fabricated on ferroelectric LiNbO3 substrate for studying magnetic anisotropy induced by the heterojunction. AIP Advances, 2018, 8, 056411.	1.3	4
43	Heterojunction-induced magnetic anisotropy and magnetization reversal of Ni wires on LiNbO3 substrate. Journal of Magnetism and Magnetic Materials, 2018, 453, 107-113.	2.3	11
44	A Study for Sensitivity Improvement of 3-D Lab-on-a-CD-Based Immunosensor. Electronics and Communications in Japan, 2018, 101, 61-68.	0.5	0
45	A 5.8 GHz Microwave Applicator by Post-Wall Waveguide. , 2018, , .		0
46	Fabrication of Integrated PTFE-Filled Waveguide Butler Matrix for Short Millimeter-Wave by SR Direct Etching. IEICE Transactions on Electronics, 2018, E101.C, 416-422.	0.6	3
47	Study on fabrication of molecular sensing system using higherâ€order nanostructure for environmental analysis and food safety. Electronics and Communications in Japan, 2018, 101, 38-44.	0.5	3
48	Study on Fabrication of Molecular Sensing System using Higher-order Nanostructure for Environmental Analysis and Food Safety. IEEJ Transactions on Sensors and Micromachines, 2018, 138, 191-197.	0.1	0
49	On-chip synthesis of ruthenium complex by microwave-induced reaction in a microchannel coupled with post-wall waveguide. Sensors and Actuators B: Chemical, 2017, 242, 384-388.	7.8	9
50	Interdigital transducer generated surface acoustic waves suitable for powder transport. Advanced Powder Technology, 2017, 28, 491-498.	4.1	1
51	Caltrop particles synthesized by photochemical reaction induced by X-ray radiolysis. Journal of Synchrotron Radiation, 2017, 24, 653-660.	2.4	15
52	Caltrop cupric oxide particles synthesized by X-ray photochemical reaction. , 2017, , .		0
53	Synthesis and immobilization of cupric oxide particles using X-ray raiolysis. , 2017, , .		0
54	Fabrication of higher order nanostructure for molecular sensing. , 2017, , .		0

4

Акілови Үамадисні

#	Article	IF	CITATIONS
55	Gold Nanoparticles Based Nanosensors/Nanobeacons Fabricated by Bottom-up Method for Surface Enhanced Raman Scattering. Bunseki Kagaku, 2017, 66, 919-923.	0.2	2
56	Control of Domain Structure in Artificial Ni Wires Fabricated on an LiNbO <sub>3</sub> Substrate. IEEE Transactions on Magnetics, 2017, 53, 1-4.	2.1	9
57	Biofilm Formation Behaviors on Graphene by <i>E. coli</i> and <i>S. epidermidis</i> . ECS Transactions, 2017, 80, 1167-1175.	0.5	6
58	The gold nanotag for on-dose authentication to prevent fake drugs. , 2017, , .		0
59	Control of domain structure in artificial Ni wires fabricated on a LiNbO <inf>3</inf> substrate. , 2017, ,		0
60	Fabrication of waveguide butler matrix for short millimeter-wave using X-ray lithography. , 2017, , .		1
61	Magnetoresistance of NiCu Micro-wires Fabricated on a LiNbO <sub>3</sub> Substrate. IEEJ Transactions on Fundamentals and Materials, 2017, 137, 487-488.	0.2	0
62	Synthesis of Cupric Particles Induced by X-ray Radiolysis. IEEJ Transactions on Electronics, Information and Systems, 2017, 137, 400-405.	0.2	0
63	A study for Sensitivity Improvement of 3-D Lab-on-a-CD based Immunosensor. IEEJ Transactions on Electronics, Information and Systems, 2017, 137, 418-423.	0.2	0
64	Study on Microfabrication of Polytetrafluoethylene using X-ray-induced Pyrochemical Anisotropic Etching. IEEJ Transactions on Sensors and Micromachines, 2017, 137, 417-421.	0.1	0
65	One-Step Synthesis of Copper and Cupric Oxide Particles from the Liquid Phase by X-Ray Radiolysis Using Synchrotron Radiation. Journal of Nanomaterials, 2016, 2016, 1-16.	2.7	18
66	Rapid X-ray Fabrication of Microstructured Polytetrafluoroethylene Substrates by Anisotropic, Pyrochemical Microetching. Journal of Photopolymer Science and Technology = [Fotoporima Konwakai Shi], 2016, 29, 403-407.	0.3	7
67	Anisotropic pyrochemical microetching of poly(tetrafluoroethylene) initiated by synchrotron radiation-induced scission of molecule bonds. Applied Physics Letters, 2016, 108, .	3.3	22
68	Synthesis of metallic nanoparticles through X-ray radiolysis using synchrotron radiation. Japanese Journal of Applied Physics, 2016, 55, 055502.	1.5	21
69	Synthesis of nanoparticles through x-ray radiolysis using synchrotron radiation. , 2016, , .		1
70	Dielectrophoresis-enabled surface enhanced Raman scattering of glycine modified on Au-nanoparticle-decorated polystyrene beads in micro-optofluidic devices. Colloids and Surfaces A: Physicochemical and Engineering Aspects, 2016, 507, 118-123.	4.7	10
71	Fabrication of higher order three-dimensional layer stack nanostructure for molecular detection and electrode. , 2016, , .		0
72	Dielectrophoresis-enabled surface enhanced Raman scattering on gold-decorated polystyrene microparticle in micro-optofluidic devices for high-sensitive detection. Sensors and Actuators B: Chemical, 2016, 230, 94-100.	7.8	27

Акілови Үамадисні

#	Article	IF	CITATIONS
73	Real-space observation of magnetic vortex core gyration in a magnetic disc both with and without a pair tag. Japanese Journal of Applied Physics, 2016, 55, 023002.	1.5	7
74	Highly sensitive detection and stochastic analysis of magnetization agitation induced in a single layered magnetic wire. Journal of Magnetism and Magnetic Materials, 2016, 401, 9-15.	2.3	1
75	Point-Contact Spectroscopy of Heavy Fermion Compounds CeCu6 and CeAl3 in Magnetic Field. Physics Procedia, 2015, 75, 296-302.	1.2	2
76	Fabrication of a Dihedral Corner Reflector Array for a Floating Image Manufactured by X-ray Lithography Using Synchrotron Radiation. Transactions of the Japan Institute of Electronics Packaging, 2015, 8, 23-28.	0.4	6
77	Surface-enhanced Raman scattering active gold nanostructure fabricated by photochemical reaction of synchrotron radiation. Materials Chemistry and Physics, 2015, 160, 205-211.	4.0	19
78	Trial fabrication of PTFE-based E-plane waveguide coupler for short millimeter-wave by SR etching. , 2015, , .		0
79	Fabrication and evaluation of Dihedral Corner Reflector Array for floating image manufactured by synchrotron radiation. , 2015, , .		1
80	Application of gold nanoparticle self-assemblies to unclonable anti-counterfeiting technology. , 2015, , .		6
81	Surface-enhanced Raman spectroscopy using a coffee-ring-type three-dimensional silver nanostructure. RSC Advances, 2015, 5, 1378-1384.	3.6	33
82	Fabrication of SERS active noble metallic nanostructure by synchrotron radiation induced photochemical reaction. , 2015, , .		0
83	On-chip integration of novel Au electrode with a higher order three-dimensional layer stack nanostructure for surface-enhanced Raman spectroscopy. RSC Advances, 2015, 5, 73194-73201.	3.6	9
84	Cu pattern etching by oxygen gas cluster ion beams with acetic acid vapor. , 2014, , .		0
85	Coupled oscillations of vortex cores confined in a ferromagnetic elliptical disk. Physical Review B, 2014, 90, .	3.2	14
86	Broadband spectroscopy of magnetic response in a nano-scale magnetic wire. Journal of Magnetism and Magnetic Materials, 2014, 364, 34-38.	2.3	3
87	J2240102 Proposal of Powder Feeder driven by Surface Acoustic Wave. The Proceedings of Mechanical Engineering Congress Japan, 2014, 2014, _J2240102J2240102	0.0	Ο
88	Powder Transport by Surface Acoustic Wave Actuator using Bragg Reflection. IEEJ Transactions on Electronics, Information and Systems, 2014, 134, 1934-1935.	0.2	0
89	Microfluidic devices with three-dimensional gold nanostructure for surface enhanced Raman scattering. , 2013, , .		0
90	Optofluidic Devices with Surface-Enhanced Raman Scattering Active Three-Dimensional Gold Nanostructure. Japanese Journal of Applied Physics, 2013, 52, 06GK12.	1.5	18

#	Article	IF	CITATIONS
91	Progress in Time-Resolved Photoemission Electron Microscopy at BL25SU, SPring-8: Radiofrequency Field Excitation of Magnetic Vortex Core Gyration. Japanese Journal of Applied Physics, 2012, 51, 128001.	1.5	6
92	Quasi-omnidirectional electrical spectrometer for studying spin dynamics in magnetic tunnel junctions. Review of Scientific Instruments, 2012, 83, 024710.	1.3	4
93	Specific Heat Study of the Non-centrosymmetric Superconductor LaPt <sub>3</sub> Si in Magnetic Fields. Journal of Physics: Conference Series, 2012, 400, 022079.	0.4	5
94	Differential Paramagnetic Effect of Non-Centrosymmetric Superconductor LaPt3Si. Journal of the Physical Society of Japan, 2012, 81, SB017.	1.6	1
95	Spin Torque Diode Spectroscopy of Quantized Spin Wave Excited in a Magnetic Tunnel Junction. IEEE Transactions on Magnetics, 2012, 48, 2816-2819.	2.1	6
96	Temperature estimation in a ferromagnetic Fe–Ni nanowire involving a current-driven domain wall motion. Journal of Physics Condensed Matter, 2012, 24, 024201.	1.8	16
97	Progress in Time-Resolved Photoemission Electron Microscopy at BL25SU, SPring-8: Radiofrequency Field Excitation of Magnetic Vortex Core Gyration. Japanese Journal of Applied Physics, 2012, 51, 128001.	1.5	7
98	Broadband Ferromagnetic Resonance of Micron-Scale Iron Wires Using Rectifying Effect. IEEE Transactions on Magnetics, 2011, 47, 1587-1590.	2.1	0
99	Microscopic theory of diffusive spin current with spin-orbit interaction. Physical Review B, 2011, 83, .	3.2	6
100	Time evolution of spin accumulation induced from electric field in ferromagnet. Journal of Applied Physics, 2011, 109, 07C901.	2.5	1
101	High-order standing spin wave modes in Fe <sub>19</sub> Ni <sub>81</sub> micron wire observed by homodyne method. Journal of Physics: Conference Series, 2011, 266, 012113.	0.4	2
102	Detection of ferromagnetic resonance in a single-crystalline Fe wire using a rectifying effect. Journal of Physics: Conference Series, 2011, 266, 012013.	0.4	1
103	Domain wall propagation in single crystalline iron wires. Journal of Physics: Conference Series, 2011, 266, 012024.	0.4	4
104	Detection of vortex-core dynamics using current-induced self-bistable rectifying effect. Journal of Physics: Conference Series, 2011, 266, 012080.	0.4	1
105	Magnetic-field modulation of the Josephson effect between polycrystalline CeCu2Si2and Al. Journal of Physics: Conference Series, 2011, 273, 012086.	0.4	1
106	Electrical detection of vortex states in a ferromagnetic disk using the rectifying effect. Journal of Applied Physics, 2011, 109, 07D306.	2.5	9
107	Spin current driven by thermal gradient. AIP Conference Proceedings, 2011, , .	0.4	0
108	Electric spectroscopy of vortex states and dynamics in magnetic disks. Physical Review B, 2011, 84, .	3.2	31

Ακινοβύ Υλαμασματι

#	Article	IF	CITATIONS
109	Giant magnetoresistance effect detection of magnetization reversal in single crystalline nanowires. Journal of Physics: Conference Series, 2010, 200, 042028.	0.4	1
110	Asymmetric Domain Wall Propagation in a Giant Magnetoresistance-Type Wire with Oscillating Interlayer Exchange Coupling. Applied Physics Express, 2010, 3, 093004.	2.4	6
111	Nonlinear Vortex Motion Induced by the Simultaneous Application of RF and DC Currents in a Micron-Sized <formula formulatype="inline"><tex Notation="TeX"&gt;\$hbox{Fe}_{19}hbox{Ni}_{81}\$ </tex </formula> Disk. IEEE Transactions on Magnetics. 2010. 46. 1994-1997.	2.1	3
112	Magnetization reversal and wall propagation velocity in single-crystalline and polycrystalline Fe wires. Physical Review B, 2010, 81, .	3.2	9
113	Detection of Nonlinear Spin Dynamics in Artificial Magnets Using Rectification of Planar Hall Effect. Journal of the Magnetics Society of Japan, 2010, 34, 73-77.	0.9	0
114	Anomalous Hall voltage rectification and quantized spin-wave excitation induced by simultaneous application of dc and rf currents in a single-layered <mml:math xmlns:mml="http://www.w3.org/1998/Math/MathML" display="inline"&gt;<mml:mrow><mml:mrow><mml:mrow><mml:mtext>Ni</mml:mtext></mml:mrow><mml:mrow wice_Dburged_Beginstrees.com</mml:mrow </mml:mrow></mml:mrow></mml:math 	3.2 /> < mml:mi	23 1>81
115	wire. Physical Review B, 2009, 79, . Magnetic field dependence of rectification radio frequency current flowing through a single layered ferromagnetic wire. Journal of Applied Physics, 2009, 105, 07D301.	2.5	13
116	Direct effects of protein S in ameliorating acute lung injury. Journal of Thrombosis and Haemostasis, 2009, 7, 2053-2063.	3.8	25
117	Current manipulation of a vortex confined in a micron-sized Fe19Ni81 disk. Applied Physics Letters, 2009, 95, 122506.	3.3	12
118	Broadband ferromagnetic resonance of <mml:math xmlns:mml="http://www.w3.org/1998/Math/MathML" display="inline"&gt;<mml:mrow><mml:msub><mml:mrow><mml:mtext>Ni</mml:mtext></mml:mrow><mml:mrow using a rectifying effect. Physical Review B, 2008, 78, .</mml:mrow </mml:msub></mml:mrow></mml:math 	v> < <mark>3:2</mark> ml:mi	า>89
119	Effect of ferromagnetism on AB oscillations in a normal-metal ring. Physical Review B, 2008, 77, .	3.2	6
120	Observation of a bias-dependent constrained magnetic wall in a Ni point contact. Physical Review B, 2008, 78, .	3.2	7
121	A silicon metal-oxide-semiconductor field-effect transistor Hall bar for scanning Hall probe microscopy. Review of Scientific Instruments, 2008, 79, 083703.	1.3	2
122	DC electrical response and impedance change induced by a microwave signal in a patterned ferromagnetic wire. , 2008, , .		0
123	Self-homodyne rf demodulator using a ferromagnetic nanowire. Applied Physics Letters, 2007, 90, 212505.	3.3	20
124	The rectification of radio-frequency signal by magnetic domain wall in a single-layered ferromagnetic nanowire. Applied Physics Letters, 2007, 91, 132509.	3.3	14
125	Rectification of radio frequency current in ferromagnetic nanowire. Applied Physics Letters, 2007, 90, 182507.	3.3	64
126	Magnetic properties of nanometer-scale FeNi antidot array system. Journal of Magnetism and Magnetic Materials, 2007, 310, e792-e793.	2.3	5

Ακινοβύ Υλαμασματι

#	Article	IF	CITATIONS
127	Galvanomagnetic Effect in Tri-layered Py/Cu/Py Ring Structures. Journal of the Magnetics Society of Japan, 2007, 31, 77-80.	0.4	1
128	Domain wall resistance in FePt wire with perpendicular magnetic anisotropy. Journal of Applied Physics, 2006, 99, 08G520.	2.5	8
129	Reduction of Threshold Current Density for Current-Driven Domain Wall Motion using Shape Control. Japanese Journal of Applied Physics, 2006, 45, 3850-3853.	1.5	40
130	Effect of Joule heating in current-driven domain wall motion. Applied Physics Letters, 2005, 86, 012511.	3.3	148
131	Real-Space Observation of Current-Driven Domain Wall Motion in Submicron Magnetic Wires. Physical Review Letters, 2004, 92, 077205.	7.8	883
132	Magnetic properties of the dense Kondo compound PrSn3. Journal of Magnetism and Magnetic Materials, 2001, 226-230, 142-144.	2.3	3
133	Cylindrical Fermi surfaces in rare-earth and actinide compounds. Physica B: Condensed Matter, 2000, 281-282, 758-760.	2.7	1
134	Heavy electron mass and the Kondo effect in PrSn3. Physica B: Condensed Matter, 2000, 281-282, 126-127.	2.7	2
135	Magnetic and Electrical Properties in a Dense Kondo Compound PrSn3. Journal of the Physical Society of Japan, 2000, 69, 3983-3995.	1.6	31
136	Two Dimensional Fermi Surfaces of CePtAs and CePtP Studied by the de Haas-van Alphen and Magnetoresistance Experiments. Journal of the Physical Society of Japan, 1999, 68, 3615-3622.	1.6	17
137	Effect of Monoclonal Anti-Human GP130 Antibody (GPX7) on Bone Turnover in Normal and Ovariectomized Rats. Calcified Tissue International, 1998, 62, 227-236.	3.1	7
138	Microchimerism and graft acceptance: cardiac allografting with multiple minor histocompatibility antigen differences. Transplantation Proceedings, 1996, 28, 1293-4.	0.6	0
139	Microchimerism and graft acceptance: cardiac allograft acceptance following antiadhesion molecules antibody therapy. Transplantation Proceedings, 1996, 28, 1370-1.	0.6	1
140	Temperature dependence of growth rate for diamonds grown using a hot filament assisted chemical vapor deposition method at low substrate temperatures. Applied Physics Letters, 1994, 64, 1306-1308.	3.3	22
141	Inhibitory effect of edible plant extracts on 12-O-tetradecanoylphorbol–13-acetate-induced ear oedema in mice. Phytotherapy Research, 1993, 7, 185-189.	5.8	48
142	Activation of adenylate cyclase by islet amyloid polypeptide with COOH-terminal amide via calcitonin gene-related peptide receptors on rat liver plasma membranes. Diabetes, 1990, 39, 875-877.	0.6	61
143	Glucose stimulates insulin release without altering cyclic AMP production or inositolphospholipid turnover in freshly obtained human insulinoma cells. Biochemical and Biophysical Research Communications, 1987, 145, 263-268.	2.1	8
144	Lowâ€noise properties of unbiased evenâ€harmonic Josephson mixers. Journal of Applied Physics, 1985, 57, 2099-2102.	2.5	3

#	Article	IF	CITATIONS
145	Pharmacokinetics of nifedipine and prediction of plasma concentration on essential hypertensive patients. Kobe Journal of Medical Sciences, 1985, 31, 133-44.	0.2	2
146	Roentgenographic examination of symptoms involving adhesion between gall-bladder and duodenum. Gastroenterologia Japonica, 1970, 5, 182-182.	0.3	0
147	Intensity modulated moire and its intensity-phase analysis. , 0, , .		0